exhibits a red shift from 460 to about 620 nm.[16] The difference between the two proteins may reside in the different number of cyanide anions bound to the metal. The additional cyanide in the transferrin complex suggested by our data would impart one more negative charge to the metal center, hence reducing the Lewis acidity of the iron in transferrin relative to the dioxygenase.

Analysis of the g factors of model compounds and proteins indicates that the complexes fall into two categories (Table I). The Schiff base complexes in the first category are similar to the type O low-spin heme complexes categorized by Blumberg and Peisach[30] where, according to Bohan,[27] g_x is positive and g_y and g_z are negative with the unpaired electron located in a d_{xz} orbital ($\mu > 0$). In the Schiff base complexes the adduct ligands are coordinated trans to one another and perpendicular to the plane of the chelate ring of the base, a situation analogous to heme. The second category consists of the commonly employed model compound for transferrin FeEHPG,[23,25,31] dioxygenase, and transferrin, all having positive g factors and the unpaired electron in a d_{xy} orbital ($\mu < 0$). In contrast to the first category, the cyanide ligands of the dioxygenase and transferrin complexes are thought to be cis.

The values of the axial crystal field parameter μ of the compounds in Table I are rather large, falling in the range 2500-4400 cm^{-1} where λ is taken as $\sim$400 cm^{-1}.[32] A significant lifting of the t_{2g} d-orbital degeneracy is required for the observation of electron paramagnetic resonance.[33] The complexes are all highly rhombic in their crystal fields as reflected in the values of R/μ. Transferrin has the lowest "symmetry" with $R/\mu = 0.63$, a value approaching the theoretical limit of 0.67 for rhombic symmetry.[27]

Acknowledgment. This work was supported by National Institutes of Health Grant GM-20194. We thank Judith Harrison for writing the driver program for the Hamiltonian matrix calculation and Dr. Lawrence Que, Jr., for helpful comments regarding the visible spectral data.

(30) Blumberg, W. E.; Peisach, J. In *Bioinorganic Chemistry*; Gould, R., Ed.; Advances in Chemistry Series 100; American Chemical Society: Washington, DC, 1971; pp 271-291.
(31) Patch, M. G.; Simolo, K. P.; Carrano, C. J. *Inorg. Chem.* **1983**, *22*, 2630-2634.
(32) Griffith, J. S. *The Theory of Transition Metal Ions*; Cambridge University: Cambridge, U.K., 1961; p 437.
(33) Wertz, J. E.; Bolton, J. R. *Electron Spin Resonance*; McGraw-Hill: New York, 1972; pp 314-323.

Infrared Spectra and Structures of Lithium-Benzene and Lithium-Dibenzene Complexes in Solid Argon

Laurent Manceron[†] and Lester Andrews*[‡]

Contribution from the Laboratoire de Spectrochimie Moléculaire (CNRS, UA508), Université Pierre et Marie Curie, 4 place Jussieu, 75005 Paris, France, and the University of Virginia, Chemistry Department, Charlottesville, Virginia 22901. *Received June 1, 1987*

Abstract: Cocondensation of lithium and sodium atoms with benzene diluted in argon produced new infrared absorptions attributable to mono- and dibenzene complexes in the case of lithium but nothing with sodium. Isotopic studies (^{6}Li, ^{7}Li, C_6H_6, C_6D_6) of the observed fundamentals suggest that the Li position in the monobenzene complex is axial and that the ligand is distorted from 6-fold symmetry. The symmetric ring-breathing mode, forbidden for C_6H_6, gives a strong 924-cm^{-1} absorption with a 2-cm^{-1} lithium isotopic shift for LiC_6H_6. The dibenzene species exhibits a strong ring-breathing mode at 901 cm^{-1}, and motions of the two spectroscopically equivalent benzene ligands are coupled. Interaction of ring-breathing and Li-ring stretching modes indicates a significant electronic interaction between lithium and benzene in these complexes.

Lithium forms insertion compounds of formula LiC_6 with graphite as well as complexes with large benzenoid polycyclic molecules.[1,2] These compounds, owing to their physical properties as conducting materials, have been the subject of experimental and theoretical investigations; several of their physical properties (C-C distance increase and ^{7}Li magnetic coupling) have been discussed in terms of charge transfer of the alkali valence electron, the extent of which is still a matter of current controversy. Recently two theoretical studies[3,4] have been devoted to interaction between Li and C_6H_6, hoping to attain better understanding of a "less complex" system than large aromatic molecules. In the course of our investigation of alkali metal atom reactivity with unsaturated hydrocarbons in solid argon, it was desired to determine if aromatic molecules form strong complexes with Li, as do alkenes[5] and alkynes.[6] Here is reported an infrared study of the interaction between Li atoms and benzene.

Experimental Section

The cryogenic refrigeration system, vacuum vessel, alkali-atom source, and experimental techniques have been described elsewhere.[7] Isotopically enriched samples of lithium metal, 99.99% ^{7}Li and 95.6% ^{6}Li (ORNL), and natural sodium metal (Baker and Adamson, 99.9%) were evaporated directly from a heated Knudsen cell. High-purity benzene (Baker, spectroscopic grade) and benzene-d_6 (MSD, 98% D) were frozen, thawed, and outgassed at liquid nitrogen temperature before use. Argon gas (99.995%, Air Products) was used without purification. Gaseous benzene/argon mixtures were deposited at about 2 mmol/h simultaneously with the alkali-metal beam on a CsI (mid-IR) or on a polished copper block (Raman). The lithium concentration was modified by varying the temperature of the Knudsen effusion cell, resulting in a 10-fold change in metal vapor pressure. The highest Li/Ar concentration used here is estimated at 1/600.

[†] Université Pierre et Marie Curie.
[‡] University of Virginia.

(1) Brooks, J. J.; Rhine, W. E.; Stucky, G. D. *J. Am. Chem. Soc.* **1972**, *94*, 7339; **1975**, *97*, 737. Rhine, W. E.; Davis, J.; Stucky, G. D. *J. Am. Chem. Soc.* **1975**, *97*, 2079.
(2) Badauski, D.; Broser, W.; Hecht, H. J.; Rewicki, D.; Dietrich, H. *Chem. Ber.* **1979**, *112*, 1380.
(3) Jebli, R.; Volpilhac, G. F.; Hoarau, J.; Achard, F. *J. Chem. Phys.* **1984**, *81*, 13.
(4) Morton-Blake, D. A.; Corish, J.; Beniere, F. *Theor. Chim. Acta* **1985**, *68*, 389.
(5) Manceron, L.; Andrews, L. *J. Phys. Chem.* **1986**, *90*, 4514.
(6) Manceron, L.; Andrews, L. *J. Am. Chem. Soc.* **1985**, *107*, 563.
(7) Andrews, L. *J. Chem. Phys.* **1968**, *48*, 972.

0002-7863/88/1510-3840$01.50/0

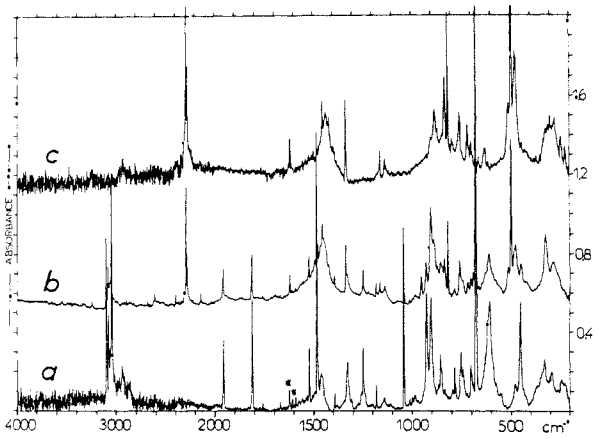

Figure 1. IR spectra recorded after deposition of lithium atoms and benzene/argon mixtures (0.5 mmol estimated amount). (a) $Li/C_6H_6/Ar$ (1.2/1/1000). (b) $Li/C_6H_6/C_6D_6/Ar$ (1.2/0.8/0.8/1200). (c) $Li/C_6D_6/Ar$ (1.2/1/1000). (*) Designates water impurity absorptions.

Mid-IR spectra (4000–200 cm^{-1}) were recorded with a Beckman IR 12 or a Perkin-Elmer 983 instrument and data station. The IR spectra presented here were processed against a background spectrum collected with the bare CsI window and then baseline corrected to compensate for matrix light scattering. Frequency accuracy is ±0.5 cm^{-1} with spectral slitwidths of 4–1.2 cm^{-1} in the product band regions. Raman spectra, recorded on a PHO Coderg instrument, were obtained by excitation with a Spectra Physics Ar^+ laser with interference filters; blank or metal-containing sample spectra are obtained in the same experimental conditions by screening out the metal on half the matrix sample and by focusing the laser beam on either the metal-containing or the metal-free part of the sample.

Results

When Li atoms were codeposited with benzene (Bz) diluted in argon, IR product bands attributable to at least three different species were observed and differentiated by varying the metal and Bz concentrations. This stands in sharp contrast to experiments with Na, which gave no evidence for product formation. Such an absence of strong interaction between sodium and Bz at the atom–molecule level has already been noted in solid Bz/alkali-metal deposits.[8,9] For instance, Moore et al.[9] reported that heavier, more electropositive K, Rb, and Cs were needed to produce M^+Bz^- ion pairs or other radical anionic species in neat Bz.

Figure 1 presents IR absorptions observed for Li + Bz diluted in argon. Absorptions were observed for two species, which were detected at the highest metal dilutions used here (Li/Ar = 1/5000 molar ratio) but whose relative intensities vary with the benzene concentration or the deposition temperature of the sample. For these two species, LiC_6H_6 and $Li(C_6H_6)_2$, stoichiometries have been clearly established on the basis of marked concentration dependence and confirmed by observation of isotopic patterns in $C_6H_6 + C_6D_6$ mixtures. A third species (labeled X) appears for high Li concentrations (Li/Ar > 1/600) when the Bz concentration is lower than or equal to 1/500. Its formation conditions definitely indicate a higher Li dependence than LiC_6H_6, and a $Li_2C_6H_6$ stoichiometry is most likely. Another species, Y, characterized by only two bands in these experiments, appears in argon samples annealed to 35 K, in heavily concentrated samples, and in lithium-rich neat Bz deposits. These two latter species will not be discussed here. In this section we will present evidence for identification of the LiC_6H_6 and $Li(C_6H_6)_2$ species and describe their spectral characteristics. The positions of the different observed absorptions are given in Table I for ^6Li, ^7Li and C_6H_6, C_6D_6 precursors; assignments, which are not straightforward for such large polyatomic systems, will be discussed in the following section on the basis of different isotopic shifts and possible mode mixing between motions belonging to identical symmetry classes.

(8) McCullough, J. D.; Duley, W. W. *Chem. Phys. Lett.* **1972**, *15*, 240.
(9) Moore, J.; Thornton, C.; Collier, W. B.; Delvin, J. P. *J. Phys. Chem.* **1981**, *85*, 350.

Table I. Infrared Absorptions (cm^{-1}) Observed for Products of Lithium-7[a] (Lithium-6 Values, When Different, Are Indicated in Parentheses) and Normal and Deuteriated Benzene[b]

identity	Li + C_6H_6 (^6Li)	Li + C_6D_6 (^6Li)	$C_6H_6 + C_6D_6$, additional signals
$Li(C_6H_6)_2$	3060, vw	2255, vw	
	3048, w		
	1480, m, broad	1435, m, broad	
	1138, w		
	984, vw		949 (949.5)
		883, m (885)	887 (889)
	901, s (906)		
		832, m (834)	845 (847)
	327, w (344)	365, w (379)	
	290, w (305)	318, m (326)	301 ?
LiC_6H_6	3055, w	2234, vw	
	1458, w, broad	1425, w, broad	
	1325, m	1217, w	
		1134, w	
	990, vw		
	924, s (926)	883, s (885)	
		757, m	
	701, w, sh		
	607, s (610)	478, s (~505)	
	451, s (483)	401, vw (421)	
		281, w (302)	
$Li_2C_6H_6$	1492	1418	
	1245		
	996		
	783	717	
	751		
	740	610	
	550	517	
		504	
Y	937	900	
	717	630	

[a] Lithium-6 values, when different, are indicated in parentheses. [b] Relative intensities are indicated by s = strong, m = medium, w = weak, vw = very weak, sh = shoulder on parent molecule absorption.

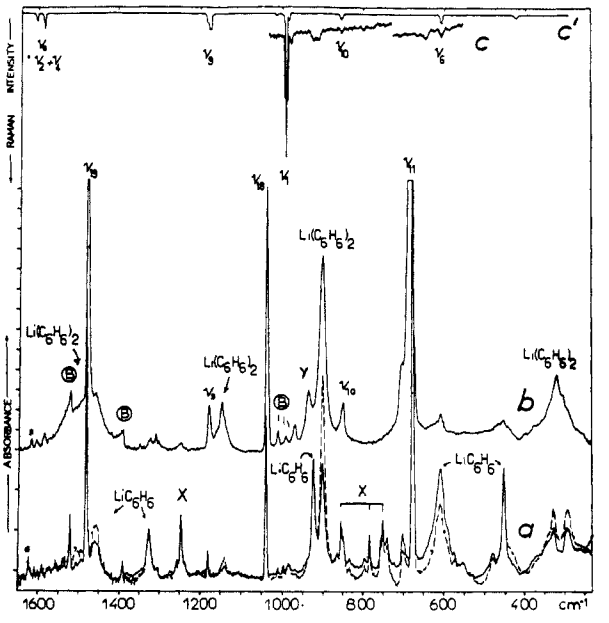

Figure 2. Comparison of IR and Raman spectra for various lithium benzene/argon samples in the 1600–250-cm^{-1} region. (a) $Li/C_6H_6/Ar$ (1.2/1/1000) (plain line after deposition, dotted line after annealing to 30–35 K). (b) $Li/C_6H_6/Ar$ (0.8/5/1000). (c) $Li/C_6H_6/Ar$ (2.4/10/1000) (exc 514.5 nm, 40-mW power). (c') C_6H_6/Ar (0.0/10/1000), same as c but not metal. B designates parent molecule combinations, (*) water impurity absorptions.

The LiC_6H_6 species is mainly characterized by three strong bands at 924, 607, and 451 cm^{-1}, two medium bands at 1458 and 1325 cm^{-1}, and a weaker band at 3055 cm^{-1} with ^7Li and C_6H_6

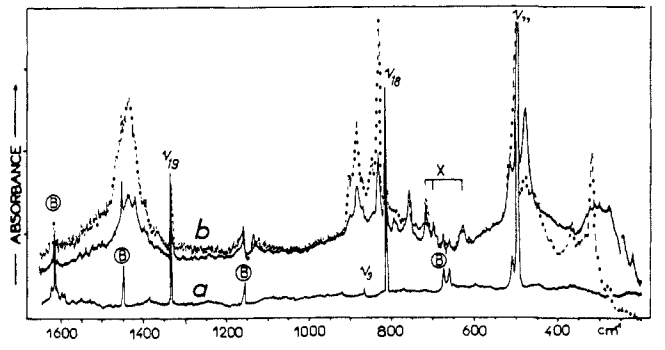

Figure 3. IR spectra of the 1600–250-cm^{-1} region for lithium + deuteriated benzene/argon samples. (a) C_6D_6/Ar (1/1000). (b) Li/C_6D_6/Ar (1.2/1/1000) (plain line after deposition, dotted line after annealing to 35 K. B designates parent molecule fundamentals and combinations.

precursors. The three stronger absorptions are the most intense product bands at low benzene (1/1000) and high lithium (1/600) molar concentrations. These bands decrease upon annealing the sample above 35 K, with growth of bands due to the dibenzene complex: likewise, a 5-fold increase in the Bz concentration causes approximately a 5-fold decrease in the relative intensities of the LiC_6H_6 versus $Li(C_6H_6)_2$ IR bands (see Figure 2).[10] The lower frequency mode displays a very large $^6Li/^7Li$ ratio (483/451 cm^{-1}) unlike the 607-cm^{-1} band, which shifts markedly upon deuterium substitution (to 478 cm^{-1}). The case of the 924-cm^{-1} band (which has a remarkable 2-cm^{-1} $^6Li/^7Li$ shift) is complicated by overlapping with $Li(C_6H_6)_2$ absorptions.

The $Li(C_6H_6)_2$ species is characterized by a very strong 901-cm^{-1} absorption (906 cm^{-1} with ^6Li) and weaker, broader, absorptions at about 1480 cm^{-1} (60 cm^{-1} full width at half maximum (FWHM)), 1138 cm^{-1} (15 cm^{-1} FWHM), and by a doublet at 327 and 290 cm^{-1}, whose components coalesce into a single broad band centered at about 319 cm^{-1} in concentrated Bz experiments. It should be mentioned that widths as well as positions of some of the other bands due to $Li(C_6H_6)_2$ are affected by concentration. In Figure 2 (traces a and b) one can see slight differences in band shapes and positions between absorptions of $Li(C_6H_6)_2$ formed upon annealing of a diluted sample or deposition of a concentrated sample. With C_6D_6, new absorptions at 1435 cm^{-1} and 365, 318 cm^{-1} are assigned to the corresponding higher and lower frequency motions of $Li(C_6D_6)_2$, but for the stronger, medium frequency bands, two absorptions appear at 883 and 832 cm^{-1} (885 and 834 cm^{-1} with ^6Li), which are present at low Bz concentration but increase with annealing and higher Bz concentration. Nevertheless, careful appraisal of the relative intensity ratio of the 883- and 832-cm^{-1} signals shows variation by a factor 1.4 upon annealing (Figure 3), from 0.8 to 0.55, in a low Bz concentration run (1/1000). This ratio also markedly decreases in highly concentrated Bz experiments but reaches a constant value of about 0.5 in samples where the LiC_6H_6 species is usually undetected. Our conclusion is that the $Li(C_6D_6)_2$ species is responsible for two absorptions at 883 and 832 cm^{-1}, but LiC_6D_6 also absorbs near 883 cm^{-1}.

This situation makes the isotopic mixture $C_6H_6 + C_6D_6$ case more intricate, since the same region contains LiC_6H_6, $Li(C_6H_6)_2$, LiC_6D_6, and $Li(C_6D_6)_2$ absorptions, as well as new bands pertaining to mixed species. Figure 4a presents a mixed-ligand experiment (C_6H_6/C_6D_6/Ar = 1/1/1200) compared with C_6H_6 and C_6D_6 (1/1000 in each case) experiments represented by the sum of the spectra obtained separately and normalized to the 901-cm^{-1} $Li(C_6H_6)_2$ band. A new signal was observed at 949 cm^{-1} in a region with no corresponding signal for only C_6H_6 and C_6D_6 products. In addition to this signal, two pronounced shoulders were observed (i) on the low-frequency side of the strong 901-cm^{-1} $Li(C_6H_6)_2$ absorption and (ii) between the weakly activated free Bz 854-cm^{-1} band and the second component of the $Li(C_6D_6)_2$ doublet at 832 cm^{-1}. The two corresponding maxima appear more clearly at 887 and 845 cm^{-1} in the difference spectrum. The other, weak absorptions below 800 cm^{-1} are due to species X ($Li_2C_6H_6$), relatively less abundant in the low concentration 1/1000 unmixed samples than in the mixture (1/600 overall Bz concentration). One could argue that the 887-cm^{-1} signal, being almost coincident with the LiC_6D_6 band at 883 cm^{-1}, could be a subtraction artifact due to a slightly different distribution between LiBz and $Li(Bz)_2$ in the two spectra. This difference indeed exists, but it is in the opposite direction (i.e., less LiBz in the mixture than in the sum of the unmixed sample) from the one that would produce such an effect, as illustrated by the negative 924-cm^{-1} LiC_6H_6 band caused by the smaller overall Bz concentration in the unmixed samples. The dimeric nature of the three, 949, 887, and 845 cm^{-1}, mixed product bands is also confirmed by their pronounced growth upon annealing (Figure 4b). Care was taken to see if these bands belong to the same species, ruling out the presence of two possible $Li(C_6H_6)_{n-x}(C_6D_6)_x$ species if $n > 2$, which would thus contradict the presumed stoichiometry of the larger species. Figure 5 presents the variation of the relative intensities of the product bands with different C_6H_6/C_6D_6 ratios. Not only does no substantial difference appear in the relative intensities of the three additional bands but also one can see (on the 949-cm^{-1} peak, which is free of overlapping) that the mixed $Li(C_6H_6)(C_6D_6)$ product peaks reach their maximum relative value for a C_6H_6/C_6D_6 ratio of 1, corresponding to the larger statistical weight for a mixed diligand species.

Since these samples are colored, attempts were made to collect their Raman spectra; Raman spectra were easy to obtain in the metal-free part of the sample, but in the metal-containing part high levels of background scattering and rapid degradation by the laser beam was a severe limitation, even with light powers as low as 50 mW and without beam-focusing devices. With the 488-nm exciting line, the sample degradation was very quick and no band was seen aside from unreacted Bz. With the 514.5-nm line, the sample degradation was slow enough to allow scanning over a sufficient frequency range; two product bands at 925 and 650 (±2) cm^{-1} were reproducibly detected by scanning at different locations in the sample (Figure 2). Given the fact that these weak signals were observed for the most concentrated Bz sample only (1/100), it is difficult to assess whether or not they belong to the same species. Nevertheless, the coincidence between the 925-cm^{-1} Raman band and the most intense 924-cm^{-1} LiC_6H_6 IR absorption is noteworthy.

Experiments run in neat Bz produced IR absorptions attributable to the $Li(Bz)_2$ species and Y; the latter species was favored by an increase in Li concentration. Although $Li(C_6H_6)_2$ absorptions were broader than those seen in argon and often overlap unreacted Bz bands, absorptions observed at 1495, 1142, 900, and 330 cm^{-1} correspond to the strongest argon values. Progressively increasing the substrate temperature indicated that $Li(Bz)_2$ slowly decomposes under vacuum between 150 and 200 K, leaving IR absorptions characteristic of Bz adsorbed on a metal film.

Discussion

Assignment of the observed IR-active motions for the different lithium/benzene complexes provides information on structures and bonding of these species. In order to simplify the notation and since it will be shown that the complexes retain a certain degree of symmetry, the description of the observed normal modes of complexed benzene will be made by reference to the similar motions of free Bz, mentioning in parentheses the symmetry class and/or Wilson's numbering of corresponding parent bands.[12]

(10) At first view, it is surprising to find an observable amount of $Li(C_6H_6)_2$ at a Bz concentration (Bz/Ar = 1/1000) that normally ensures negligible proportion of polymers for small molecules, but Bz is a bulky molecule that is likely to occupy more than one substitutional site of the argon lattice, hence yielding a higher aggregation probability than small molecules. The difficulty of isolating Bz in inert gases has already been outlined and analyzed by Brown and Person[11] and the ratio of Bz monomer to dimer can be conveniently followed on some of its fundamentals (see for instance 1039 cm^{-1}, 1041 cm^{-1} in Figure 4b).

(11) Brown, K.; Person, W. *Spectrochim. Acta Part A* **1973**, *34A*, 117.

(12) Wilson, E. .; Decius, J. C.; Cross, P. *Molecular Vibrations*; McGraw Hill: New York, 1955.

Table II. Comparison between Calculated and Observed Frequencies for LiC_6H_6 for the A_1 Block Motions, Assuming C_{6v} Geometry[a]

$^6LiC_6H_6$			$^7LiC_6H_6$			$^6LiC_6D_6$			$^7LiC_6D_6$		
$\nu_{calcd}(I)$	$\nu_{calcd}(II)$	ν_{obsd}	$\nu_{calcd}(I)$	$\nu_{calcd}(II)$	ν_{obsd}	$\nu_{calcd}(I)$	$\nu_{calcd}(II)$	ν_{obsd}	$\nu_{calcd}(I)$	$\nu_{calcd}(II)$	ν_{obsd}
3058.6	3058.6	3055	3058.6	3058.6	3055	2267.3	2267.2	2234	2267	2267	2234
925.0	926	926	922.8	923.5	924	884.2	885.5	885	881.8	882.7	883
609.0	610.4	610	607.0	608.7	607	508.9	507.3	~505	486.3	485.7	478
482.8	480.0	483	452.0	449.5	451	422.4	421.1	421	412.7	411.9	401

[a] Set (I): F_{11} = 6.18, F_{22} = 0.194 mdyn Å^{-1}, F_{33} = 0.232 mdyn Å^{-1}, F_{44} = 5.1 mdyn Å^{-1}, F_{12} = +0.18 mdyn Å^{-1}, F_{23} = 0.01 mdyn, F_{14} = 0.1 mdyn Å^{-1}. Set (II): F_{11} = 6.75, F_{22} = 0.195 mdyn Å^{-1}, F_{33} = 0.233 mdyn Å^{-1}, F_{44} = 5.1 mdyn Å^{-1}, F_{12} = −0.40 mdyn Å^{-1}, F_{23} = 0.01 mdyn, F_{14} = 0.10 mdyn Å^{-1}.

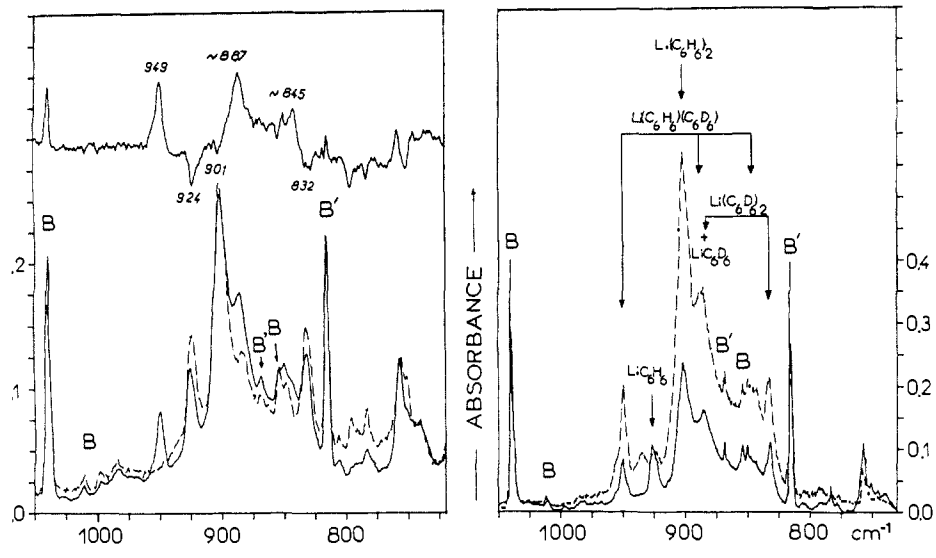

Figure 4. Expanded IR 1050–650-cm^{-1} spectra of Li + C_6H_6/C_6D_6 mixtures in solid argon. (A) Bottom solid line: C_6H_6/C_6D_6/Ar (1/1/1200) (with 2.5-cm^{-1} resolution). Dotted line: sum spectrum of two separate experiments with C_6H_6 or C_6D_6/Ar (1/1000). Top solid trace: difference spectrum of the two bottom traces. (B) Solid line: same as bottom A, but with 1.2-cm^{-1} resolution and absorbance scale × 0.5. Dotted line:b same sample after annealing to 35 K. B and B′ designate normal and deuteriated benzene absorptions.

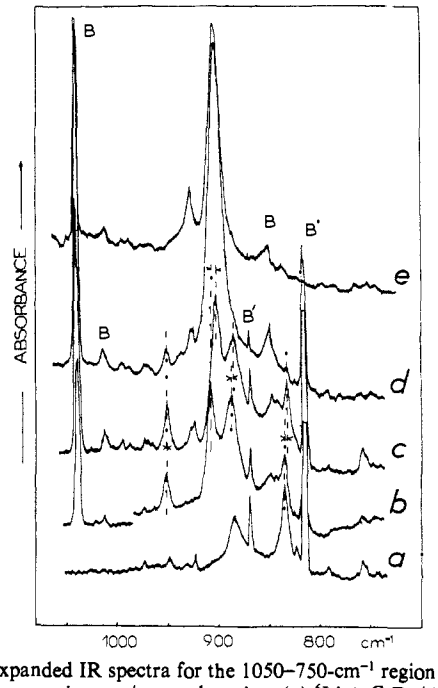

Figure 5. Expanded IR spectra for the 1050–750-cm^{-1} region for various lithium/benzene mixtures/argon deposits. (a) ^{6}Li + C_6D_6/Ar (1/200). (b) ^{6}Li + C_6D_6/Ar (0.66/0.33/200). (c) ^{7}Li + C_6D_6/C_6H_6/Ar (0.5/0.5/200). (d) ^{7}Li + C_6D_6/C_6H_6/Ar (2/0.4/200). (e) ^{7}Li + C_6H_6/Ar (0.5/200). B and B′ designate C_6H_6 and C_6D_6 absorptions. Note the small but noticeable ^{6}Li/^{7}Li shifts between b and c.

LiC_6H_6. The H/D and ^{6}Li/^{7}Li shifts on the three strongest bands of LiC_6H_6 reveal their normal-mode character in a quite straightforward manner. The large lithium isotopic shift for the 451-cm^{-1} band (32 cm^{-1}) clearly identifies a lithium–carbon stretching mode. The magnitude of this ^{6}Li/^{7}Li shift is remarkable: a Li atom vibrating against an infinite mass would have a 36-cm^{-1} ^{6}Li/^{7}Li shift or against a 78 amu point mass a 33-cm^{-1} lithium shift at this frequency by use of the harmonic approximation. This is, in any case, indicative of a bridging position for the lithium atom, which interacts with more than one carbon in the benzene ring. For a minimal symmetry reduction (C_{6v}), A_1 and E_2 metal carbon stretching modes are expected. With use of the Wilson GF method[12] and assuming six Li–C bond stretching coordinates, the G-matrix elements for the two Li–C stretching modes expressed in symmetry coordinates are

$$G(A_1)\ \mu C + \mu Li\ (1 + 2\cos\theta_o + 2\cos\theta_m + \cos\theta_p)$$

$$G(E_2) = \mu C + \mu Li\ (1 + \cos\theta_o - \cos\theta_m - \cos\theta_p)$$

where μLi and μC are the inverse masses of Li and C and θ_o, θ_m, and θ_p are the angles between C–Li "bonds" in ortho, meta, and para positions, respectively. A correct fit of the observed lithium isotopic shift for the symmetric mode, neglecting interaction with the other A_1 modes, is obtained with C–Li distance of 2.30 Å (1.82 Li–ring distance and 1.4 Å C–C distance), which compares favorably with 2.32 Å derived from crystallographic data of LiC_6 lithium–graphite intercalates.[1] In contrast, reproduction of the correct lithium effect on the antisymmetric mode would require unrealistic figures for Li–C distances (less than 1.5 Å, i.e., Li–ring distances 0.5 Å!). In case of symmetry lowering, the nonequivalence of some of the Li–C interactions should split the E_2 mode, if the 3-fold symmetry axis is lost (C_{2v}), into two components of slightly different energies, but in any case this would affect very little the relative magnitudes of the isotopic shifts, which are discussed above. The observed lithium motion is therefore assigned to the axial lithium–ring stretching mode.

The 607-cm^{-1} band of LiC_6H_6 has a small ^{6}Li/^{7}Li effect, but the magnitude of the deuterium shift identifies it as a C–H bending mode. It is slightly red-shifted with respect to the two lowest

bending modes of uncomplexed Bz ν_4 (B_{2g}) at 703 cm^{-1} (1.17 H/D ratio) and ν_{11} (A_{2u}) at 675 cm^{-1} (1.35 H/D ratio). The 607-cm^{-1} band is a good candidate for the latter mode, given the 1.27 H/D ratio and the fact that it should have the same symmetry as the observed (A_1) Li–ring stretch, as evidenced by the small mixing. The 924-cm^{-1} band of LiC_6H_6, owing to the 41-cm^{-1} H/D and 2-cm^{-1} $^6Li/^7Li$ shifts, corresponds to a carbon skeleton motion; the symmetric ring-breathing mode is the most likely possibility (corresponding to ν_1 in Bz) based on (i) its close proximity (−68 cm^{-1}), (ii) the similarity of the H/D ratios (1.0464 vs 1.0427 for free Bz), and (iii) the coincidence with the position of the strongest observed Raman band. The infrared intensity of this band demonstrates that a LiBz complex is formed with lower local symmetry than benzene.

The reasonableness of these propositions has been checked with a harmonic model for the four A_1 motions and a C_{6v} structure as a first approximation. The four symmetry coordinates used as basis set are the following:

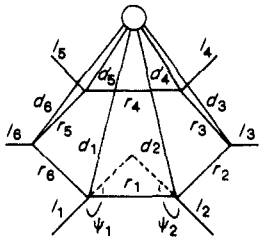

$$S_1 = 1/\sqrt{6}(r_1 + r_2 + r_3 + r_4 + r_5 + r_6)$$
$$S_2 = 1/\sqrt{6}(d_1 + d_2 + d_3 + d_4 + d_5 + d_6)$$
$$S_3 = 1/\sqrt{6}(\psi_1 + \psi_2 + \psi_3 + \psi_4 + \psi_5 + \psi_6)$$
$$S_4 = 1/\sqrt{6}(l_1 + l_2 + l_3 + l_4 + l_5 + l_6)$$

The C–C and C–H bond lengths were taken as 1.4 and 1.085 Å and the 12 carbon and hydrogen atoms were kept coplanar; a slight out-of-ring-plane bending of the six H atoms was also tested but did not lead to significant differences in the reproduction of the isotopic shifts. More sensitive was the variation of the lithium-to-ring distance. Several geometries (Li–C = 2.2, 2.3, and 2.4 Å) were also tested, and only the best overall result (for 2.3 Å) is presented. Differences were, however, small (0.5–0.8 cm^{-1}) and are not significant with respect to the necessary approximations (neglect of the anharmonicity, C_{6v} symmetry). The results presented in Table II merit comments.

For the correct reproduction of the observed isotope pattern of the two low-frequency modes, the magnitude and sign of the interaction force constant between the H wagging and Li–ring stretching coordinates can be determined unambiguously and precisely. This stems from the fact that for these two modes intercrossing occurs. The H wagging motion is situated at 607 cm^{-1}, well above the 451-cm^{-1} Li stretch, whereas in the C_6D_6 case, the order is changed. The upper component of the pair is a mixture of roughly 75% Li stretch and 25% in-phase C–D wag (with most of the intensity), and the other component is the reversed out-of-phase mixture with very little intensity.[13]

The reproduction of the trends and magnitude of the isotope shifts for the C–H and C–C modes provides, however, more than one solution. With regard to the C–C, C–H interaction, we assumed that no drastic change occurred with respect to free Bz and merely transposed the results of the recent, state of the art, calculation by Ozkabak and Goodman.[14] The observed mixture between ring breathing and Li stretch provides two solutions, which are undistinguishable as far as fitting the frequencies is concerned. Set I predicts a large weakening of the C–C force constant (18%) and a positive interaction force constant while set II predicts a smaller weakening of the C–C (10%) but a negative interaction force constant. The eigenvectors predicted by sets I and II are, of course, widely different. Thus, it should be possible to discriminate between the two sets on the basis of different relative intensity changes with the different isotopic precursors. In practice, limitations in the intensity measurements (overlapping) leave the question open. Nevertheless, we intuitively favor set I on the grounds that a shortening of the Li–C distance should cause a lengthening of the C–C distances (exemplified by the weakening of the C–C force constant compared to that of benzene in both cases) and this requires a positive sign for the S_1S_2 ineraction force constant.

The 1458-cm^{-1} band of LiC_6H_6 appears at the foot of the very strong Bz 1481 cm^{-1} fundamental (E_{1u}) but displays a very different behavior upon deuterium substitution (−35 instead of −150 cm^{-1}), which rules out this assignment. It rather suggests a red-shifted ring-stretching mode corresponding to ν_8 (E_{2g}, 1595 cm^{-1}, −42-cm^{-1} C_6D_6 shift) in free Bz. The other possibility is a blue-shifted ν_{14} (B_{2u}) type of motion (1309, −27 cm^{-1} C_6D_6 shift in free benzene). Note that these two cases would require symmetry lowerings respectively to C_{3v} and C_{2v} (see ref 12). On the other hand, the 1325-cm^{-1} band (shifting to 1134 cm^{-1} with C_6D_6) matches the characteristic isotopic shift corresponding to a perturbed ν_{19}-type ring stretching (E_{1u}, 1481 cm^{-1}, −150 cm^{-1} C_6D_6 shift for free Bz). This strong IR band is allowed for C_{6v}, C_{3v}, and C_{2v} structures. The strong 1325-cm^{-1} band is assigned to an antisymmetric ring stretching mode.

The weak 3055-cm^{-1} band for LiC_6H_6 shifts to 2234 cm^{-1} for LiC_6D_6, which clearly identifies a C–H stretching mode. The nature of the weak 701-cm^{-1} (C_6H_6) and 757-cm^{-1} (C_6D_6) absorptions is unclear in the absence of identified isotopic counterparts.

$Li(C_6H_6)_2$. $Li(C_6H_6)_2$ is mainly characterized by two intense features at 1480 and 901 cm^{-1}, which can be assigned to the same modes as the analogous 1458- and 924-cm^{-1} LiC_6H_6 bands. These ring-stretching and ring-breathing motions also present some noteworthy characteristics. First of all, it may seem surprising at first glance that the $Li(C_6H_6)_2$ ring-breathing mode appears at a lower frequency than this LiC_6H_6 mode instead of occupying an intermediate position between Bz and LiBz as does the 1480-cm^{-1} band. The position of distinct signals corresponding to $Li(C_6H_6)(C_6D_6)$ in isotopic mixtures indicates that the complex contains two presumably equivalent benzene ligands, whose ring-stretching modes are in fact coupled into two sets of vibrations (in-phase and out-of-phase), the higher set of which is either not IR active or too weak to be seen with the present conditions. Given the axial position proposed for the LiC_6H_6 complex, mutual exclusion due to the presence of an inversion center in a sandwich structure seems very likely. Among the three new signals at 949, 887, and 845 cm^{-1}, the two lower ones should involve more of the C_6D_6 moiety and the upper one at 949 cm^{-1} the C_6H_6 moiety. Comparison of the ring-breathing perturbations can be made within the normal coordinate model defined for lithium monobenzene (harmonic and C_{6v} structure approximations). It is possible to obtain good frequency fit and reproduction of the $^6Li/^7Li$ isotope effects for the C_6H_6 ligands. The C_6D_6 values do not reflect, of course, the mixing with the in-plane D bending mode discussed further (Table III). The results are compared to free Bz and $Cr(C_6H_6)_2$[15] in Table IV and show that (i) the ring-breathing force constants decrease monotonically from free C_6H_6 to $Li(C_6H_6)_2$ to LiC_6H_6, (ii) in both cases the Li perturbations are greater than that of Cr, and (iii) the large difference in the metal–ring stretching force constants reflects the very different metal to ring distances (1.61 Å with Cr, estimated 2.3 ± 0.3 Å with Li). The fact that the uncoupled ring-breathing mode comes higher than the $Li(C_6H_6)_2$ IR-active motion (A_{2u}, b in Table III, two rings out-of-phase) means that the IR-forbidden mode (A_{1g}, a in Table III, two rings in-phase) comes higher in energy (calculated in the 966-cm^{-1} vicinity to a first approximation). In other words, there is a positive interaction force constant between the two ring-breathing coordinates, or, physically speaking, lengthening of the C–C distances on one ligand favors shortening rather than lengthening the other ligand C–C distances.

(13) This incidently implies that bending the hydrogens away from the lithium and shortening of the Li–ring distance produce dipole moment changes of the same direction.

(14) Ozkabak, A. G.; Goodman, L. *J. Chem. Phys.* **1987**, *87*, 2564.

(15) Cyvin, S. J.; Brunvoll, J.; Schafer, L. *J. Chem. Phys.* **1971**, *54*, 1517.

Table III. Comparison between Calculated and Observed Frequencies for $Li(C_6H_6)_2$ A_{1g} and A_{2u} Frequencies, Assuming D_{6h} Overall Symmetry (C_{6v} for $LiC_6H_6C_6D_6$)[a]

	$^6Li(C_6H_6)_2$			$^7Li(C_6H_6)_2$			$^6Li(C_6D_6)_2$			$^7Li(C_6D_6)_2$			$^6Li(C_6H_6)C_6D_6$			$^7Li(C_6H_6)C_6D_6$		
D_{6h}	$\nu_{calcd}(I)$	$\nu_{calcd}(II)$	ν_{obsd}	$\nu_{calcd}(I)$	$\nu_{calcd}(II)$	ν_{obsd}	$\nu_{calcd}(I)$	$\nu_{calcd}(II)$	ν_{obsd}	$\nu_{calcd}(I)$	$\nu_{calcd}(II)$	ν_{obsd}	$\nu_{calcd}(I)$	$\nu_{calcd}(II)$	ν_{obsd}	$\nu_{calcd}(I)$	$\nu_{calcd}(II)$	ν_{obsd}
a	3060.2	3060.7		3060.2	3060.2		2271.8	2272.0		2271.8	2271.9		3058.9	3058.9		3058.9	3058.9	
b	3057.6	3057.6	3060	3057.6	3057.2	3060	2264.5	2264.5	2255	2264.5	2264.5	2255	2268.2	2268.2		2268.2	2268.2	
a	965.6	966.4		965.6	966.4		920.3	921.0		920.3	921.0		949.9	950.5	949.5	949.5	950.0	949
b	906.5	905.5	906	902.2	901.0	901	868.7	867.5	*885, 834	864.0	862.8	*882, 832	880.8	879.8	*889, ~847	976.5	875.5	*887, ~845
a	638.1	638.6		638.1	638.6		473.0	473.6		472.8	473.5		638.0	638.5		638.0	638.4	
b	637.9	638.4		637.7	638.2		472.9	473.5		472.2	472.7		472.5	473.6		472.5	473.1	
a	151.5	157.3		151.5	157.1		144.7	150.2		144.7	150.2		148.2	153.7		147.9	153.5	
b	327.6	328.3	+325	305.9	306.6	+308	323.1	323.6	*379, 326	302.2	302.7	*365, 318	325.4	325.9		304.1	304.7	~301

[a]Set (I): F_{11} = 6.21 mdyn Å, F_{22} = 0.162 mdyn/Å, F_{33} = 0.26 mdyn/Å, F_{44} = 5.10 mdyn Å^{-1}, F_{12} = 0.29, F_{23} = 0.01, F_{14} = 0.10, $F_{1,1'}$ = 0.60, $F_{2,2'}$ = 0.10 mdyn Å^{-1}. Set (II): F_{11} = 6.865 mdyn Å^{-1}, F_{22} = 0.162 mdyn Å^{-1}, F_{33} = 0.26 mdyn/Å, F_{44} = 5.10 mdyn Å^{-1}, F_{12} = −0.35, F_{23} = 0.01, F_{14} = 0.10, $F_{1,1'}$ = 0.62, $F_{2,2'}$ = 0.10 mdyn Å^{-1}. a = A_{1g} (inactive), b = A_{2u} (IR active), (*) split by interaction with another mode, (+) average of site split bands.

This situation is expected because in dibenzene–lithium the overall ligand perturbation is smaller than in monobenzene–lithium, and C–C bond weakenings should be in each case proportional to the metal-to-π system charge flow. This was not the case in $Cr(C_6H_6)_2$, for which the A_{1g} and A_{2u} ring-breathing motions are almost coincident (970 and 971 cm^{-1}).[15] The importance of the variation of the metal-to-π system charge flows during the ring motions is clearly evidenced by the $^6Li/^7Li$ shift on the breathing motion. It is also remarkable that the model reproduces exactly the doubling of this $^6Li/^7Li$ shift with respect to LiC_6H_6 (5 vs 2.5 cm^{-1}) in spite of the fact that the energy gap between the metal stretch and ring-breathing motions increases. This is explained logically in a centrosymmetric model without increase of the interaction force constant between these two coordinates, since the Li shifts will respectively cancel and add for the two in-phase and out-of-phase ring-breatching motions. This picture is fully supported by calculation of the small (0.5 cm^{-1}) but reproducible lithium shift on the 949-cm^{-1} band of the $Li(C_6H_6)(C_6D_6)$ species, which keeps a partial in-phase character.

The second important fact is the observation of a doublet (883–882 cm^{-1}) with C_6D_6 in place of the strong single band at 901 cm^{-1} with $Li(C_6H_6)_2$. This means that, in the case of $Li(C_6D_6)_2$, the ring breathing is coupled with another mode, which was much further away in the nondeuteriated case. It therefore means unambiguously that the "local" symmetry of the ligand is lowered from D_{6h} to the extent that another mode (certainly the hydrogen bending mode situated at 1138 cm^{-1}) belongs to the same symmetry class as the ring-breathing motion. There are two plausible candiates for its assignment: a ν_9 (E_{2g}) type of motion (1178 and 869 cm^{-1} in free C_6H_6 and C_6D_6, respectively) or a ν_{15} (B_{2u}) type (1149 and 823 cm^{-1} in free C_6H_6 and C_6D_6, respectively). The first possibility requires a D_{2h} symmetry lowering (C_{2v} locally) but fits the observed isotopic shift better than the second possible assignment, which requires a D_{3h} (C_{3v} locally) minimal symmetry lowering: it is also more consistent with the fact that another E_{2g} (ν_8 type of motion) is IR activated. Concerning the low-frequency $Li(Bz)_2$ band, it is present as a doublet in the 300-cm^{-1} region, whose two components display strong but slightly unequal $^6Li/^7Li$ isotopic shifts. Because of the large magnitude of these shifts, the doublet seems, however, likely to arise from different trapping sites inducing a splitting on the IR active, axial, Li–ring motion (B_{1u} with D_{2h} symmetry) corresponding to the one observed with LiC_6H_6 in the argon lattice rather than by observation of other, parallel to the ring planes, lithium motions.

In conclusion, for both mono- and dibenzene lithium, the new IR active vibrations are, in addition to metal–carbon stretches, skeletal vibrations corresponding to ν_1, ν_8, or ν_9 of free benzene.

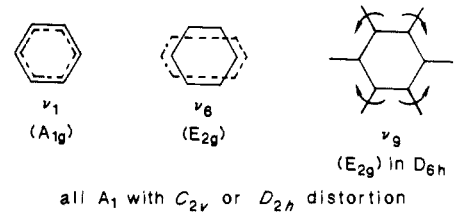

In other words, strong variations of global dipole moment occur in the complexes for normal modes where all the C–C bond distances increase or for a D_{2h} distortion of the ring. Thus, metal-to-ligand charge flows are not only related to C–C distance variations but also to C_{2v} or D_{2h} distortions of the lithium-capped benzene.

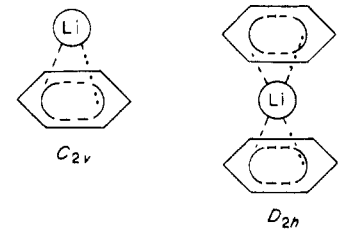

Table IV. Comparison of Some Symmetry Force Constants in Benzene, Dibenzene–Chromium, and Mono- and Dibenzene–Lithium

	free C_6H_6[a]	free C_6H_6 (this model)	LiC_6H_6[b] I	LiC_6H_6[b] II	$Li(C_6H_6)_2$[c] I	$Li(C_6H_6)_2$[c] II	$Cr(C_6H_6)_2$[d]
$F_{ring\ breath.}$, mdyn Å^{-1}	7.61	7.55	6.18	6.75	6.21	6.865	7.88
F_{wag}, mdyn Å^{-1}		0.295	0.232	0.233	0.26	0.26	0.26
F_{M-C}, mdyn Å^{-1}			0.194	0.196	0.162	0.162	1.34
$F_{M-C_6,C-C}$			0.18	−0.35	0.29	−0.35	−0.885
$F_{C-C,C-C}$							0.05

[a] Frequencies corrected for anharmonicity.[14] [b] Assuming C_{6v} structure. [c] Assuming D_{6h} structure. [d] From ref 15.

It is well known that, in a Jahn–Teller (JT) situation such as the benzenide anion (Bz^-), addition of an extra electron to one of the two unoccupied degenerate E_{2g} orbitals of free Bz will lead to a molecular distortion with the degeneracy removed. The possible carbon skeleton distortions should belong to the E_{2g} representation, i.e., Jahn–Teller active modes.[16] We believe that it is precisely such a distortion that is identified here for $Li(C_6H_6)_2$ and seems likely to occur for LiC_6H_6.[17] One could also advance that this primary mechanism (valence electron transferred to Bz) is accompanied by electron back-donation from filled E_{1g} Bz orbitals to Li $2p_x$,$2p_y$ levels (if z taken along the C_2 axis) although the former are substantially lower in energy than the latter. This can explain the consistently observed[8,9] absence of strong interaction at the atom + molecule pair level between Bz and Na where the 3p levels are more diffuse and further apart in energy from the 3s level than 2p from 2s in Li, and these interactions are less likely to occur.

ESR spectra of both free and ion-paired solvated Bz^-[18,19] have been interpreted as arising from six equivalent protons, which means that on the time scale of the ESR experiment (10^{-7} s) Bz rapidly interconverts between equivalent D_{2h} structures of minimum electronic energy. It was proposed in the case of K^+, Rb^+, or Cs^+/Bz^- ion pairs in solution that the cation occupies an average axial position yielding C_{6v} overall symmetry. The broadness of some of the observed transitions (such as the 1480 cm^{-1}, FWHM 60 cm^{-1}) is indeed conspicuous and indicates that either dynamic fluctuations occur (if the energy difference between the two possible JT distortions remain of the same order of magnitude as some vibrational transitions of the complex) or else that the potential well corresponding to the JT distortion is so shallow that multiple trapping sites inhomogeneously broaden the absorptions (as seen with halobenzene cation fluorescence studies[20]); the symmetry reduction might not be averaged out in this experiment because of the shorter time scale of the spectroscopic probe (10^{-12} s).

Conclusion

Lithium atoms spontaneously form mono- and diligand complexes with benzene diluted in an inert argon medium. This result contrasts the absence of similar product with sodium atoms as well as the failure to obtain lithium benzenide ion pairs in organic solvents.[18] In spite of the limited number of observed fundamentals, some conclusions can be reached: (i) Concerning lithium monobenzene, the lithium isotopic shift on the Li–ring stretching mode indicates an axial position for the metal, while observation of a formerly E_{2g} ring stretching mode suggests a C_{3v} or C_{2v} symmetry reduction or, in other words, a small Jahn–Teller effect. The observed coupling between the ring breathing, out-of-plane C–H bending, and Li–ring stretching modes indicates a significant electronic interaction between lithium and benzene, which was characterized by a normal coordinate analysis. (ii) Concerning lithium–dibenzene, observed mode mixing between a formerly E_{2g} (in plane) hydrogen bending mode and the perturbed mode corresponding to the totally symmetric ring breathing further specifies that, in this case, the symmetry reduction is at least D_{2h} (C_{2v} locally for a half sandwich).

Isotopic mixtures also provide evidence for intermolecular coupling between ligands during the ring-breathing motions, which is indicative of π-electron charge fluxes through the metal center in a comparable manner to that observed in lithium di- and triethylene.[5] Also, the very large intensities of the IR absorptions indicate that here, as in the case of lithium–ethylene complexes, large dipole moment variations occur during C–C stretching motions belonging to the same representation as the static distortion experienced by benzene upon complexation. Even though ligand perturbation by transition metal and lithium atoms were surprisingly similar in the case of ethylene, the effects are markedly different in the case of benzene: large perturbations on the C–C stretching modes, departure from 6-fold symmetry, and interligand ring-breathing dynamic couplings were not observed for $Cr(C_6H_6)_2$[15] or $V(C_6H_6)_2$.[21]

Acknowledgment. We gratefully acknowledge financial support from the NSF and the CNRS.

Registry No. Bz, 71-43-2; Bz-d_6, 1076-43-3; $Li(Bz)_2$, 114031-36-6; LiBz, 113997-34-5; Li_2Bz, 113997-47-0; ^{6}LiBz, 113997-35-6; ^{7}LiBz, 113997-36-7; ^{6}LiBz-d_6, 113997-37-8; ^{7}LiBz-d_6, 113997-38-9; $^6Li(Bz)_2$, 113997-39-0; $^7Li(Bz)_2$, 113997-40-3; $^6Li(Bz\text{-}d_6)_2$, 113997-41-4; $^7Li(Bz\text{-}d_6)_2$, 113997-42-5; ^{6}Li(Bz)(Bz-d_6), 113997-44-7; ^{7}Li(Bz)(Bz-d_6), 113997-45-8; Li, 7439-93-2; ^{7}Li, 13982-05-3; ^{6}Li, 14258-72-1; Na, 7440-23-5.

(16) Salem, L. *Molecular Orbital Theory of Conjugated Systems*; W. A. Benjamin: New York, 1966.

(17) Efforts to obtain further quantitative insight on the distortion of the ring reflected by small differences in C–C bond force constants are doomed by the insufficient number of observed fundamentals. Four LiC_6H_6 and four LiC_6D_6 frequencies available to parametrize the position of eight in-plane C–C stretching and C–H bending modes requires transfer of a large number of interaction force constants from free Bz, which is questionable or requires neglect of some C–C, C–H bending interactions, which is not consistent with observations.

(18) Tuttle, T. R.; Weissman, S. I. *J. Am. Chem. Soc.* **1958**, *80*, 5342.

(19) Jones, M. T.; Kuechler, T. C. *J. Phys. Chem.* **1977**, *81*, 360.

(20) Miller, T. A.; Bondybey, V. E. In *Molecular Ions*; North Holland: Amsterdam, 1983.

(21) Andrews, M. P.; Matter, S. M.; Ozin, G. A. *J. Phys. Chem.* **1986**, *90*, 744.